Extension of the Darcy–Forchheimer Law for Shear-Thinning Fluids and Validation via Pore-Scale Flow Simulations

(Article begins on next page)

10 April 2024

Extension of the Darcy-Forchheimer law for shear thinning fluids and validation via pore-scale flow simulations

Tiziana Tosco[1], Daniele L. Marchisio[2], Federica Lince[2], Rajandrea Sethi[1(*)]

[1] *DIATI – Dipartimento di Ingegneria dell'Ambiente, del Territorio e delle Infrastrutture – Politecnico di Torino, C.so Duca degli Abruzzi 24, 10129 Torino, Italy*

[2] *DISAT – Dipartimento Scienza Applicata e Tecnologia – Politecnico di Torino, C.so Duca degli Abruzzi 24, 10129 Torino, Italy*

Phone +390110907735

Fax +390110907699

Email: rajandrea.sethi@polito.it

ABSTRACT: Flow of non-Newtonian fluids through porous media at high Reynolds numbers is often encountered in chemical, pharmaceutical and food as well as petroleum and groundwater engineering and in many other industrial applications. Under the majority of operating conditions typically explored, the dependence of pressure drops on flow rate is non-linear and the development of models capable of describing accurately this dependence, in conjunction with non trivial rheological behaviours, is of paramount importance. In this work pore-scale single-phase flow simulations conducted on synthetic two-dimensional porous media are performed via computational fluid dynamics for both Newtonian and non-Newtonian fluids, and the results are used for the extension and validation of the Darcy-Forchheimer law, herein proposed for shear thinning fluid models of Cross, Ellis and Carreau. The inertial parameter β is demonstrated to be independent of the viscous properties of the fluids. The results of flow simulations show the superposition of two contributions to pressure drops: one, strictly related to the non-Newtonian properties of the fluid, dominates at low Reynolds numbers, while a quadratic one, arising at higher Reynolds numbers, is dependent on the porous medium properties. The use of pore-scale flow simulations on limited portions of the porous medium is here proposed for the determination of the macroscale averaged parameters (permeability K, inertial coefficient β and shift factor α), which are required for the estimation of pressure drops via the extended Darcy-Forchheimer law. The method can be applied for those fluids which would lead to critical conditions (high pressures for low permeability media and/or high flow rates) in laboratory tests.

KEYWORDS: *Darcy-Forchheimer law; shear thinning fluid; Computational Fluid Dynamics; pore-scale simulations; non-Newtonian flow.*

Introduction

A wide range of industrial applications involve the flow of non-Newtonian fluids through porous media. In particular, shear thinning solutions of biopolymers are often used in petroleum engineering to enhance oil recovery, thanks to their effect on reducing instabilities of the displacement front (Sethi 2011; Muskat and Wyckoff 1937; Auradou et al. 2008; Zeinijahromi et al. 2012). Also, many processes in food and chemical industry involve in-line filtration of fluids with complex rheological properties (e.g., milk, most liquid food, oil, blood, etc.) (Lee et al. 2006). Deep filtration in granular porous media is used in other specific applications, like distillation towers and fixed bed reactors (Liu and Masliyah 1998), biomedical separation devices (Rashidi et al. 2011) and ceramic foams for air filtration (Innocentini et al. 1999). Moreover, recent applications in environmental cleanup technologies involve the use of shear thinning polymeric suspensions as carrier fluids for the injection of iron nanoparticles into the subsurface (Tosco and Sethi 2010; Dalla Vecchia et al. 2009; Zhong et al. 2011; Tosco et al. 2012). In all abovementioned applications, it is of paramount importance to correctly predict the pressure drop resulting from non-Newtonian fluid flow through the porous medium. In most cases, the problem can be solved at the macroscale, using extended formulation of the Darcy law (Pearson and Tardy 2002) or solving the transient flow using similarity solutions (Ciriello and Di Federico 2012), at the micro-scale, using pore-network models or realistic pore-scale models (Blunt 2001), or adopting hybrid models which couple pore and continuum scales (Battiato et al. 2011).

The Darcy law (Darcy 1856) is the most widely used phenomenological equation for describing steady-state flow of Newtonian fluids through porous media at small Reynolds numbers, when the relationship between hydraulic gradient and fluid velocity can be modeled by a linear term only. However, when increasing the Reynolds number non-linearities arise. The origin of this non-linear behavior can be attributed to different phenomena, namely micro-scale drag forces (Hassanizadeh and Gray 1987), inertial effects (Levy et al. 1999) and low Reynolds number turbulence (Dybbs and Edwards 1984), which may arise at the solid-liquid interface for Reynolds numbers in the order of one or higher. Empirical laws were proposed which include the linear term, and one or more

additional higher-order terms, corresponding to a series expansion of the unknown function expressing the dependence of pressure drop on flow rate, truncated at a certain order. Among these phenomenological laws, the Darcy-Forchheimer law (Forchheimer 1901; Muskat and Wyckoff 1937) introduces an additional quadratic term for the dependence of the hydraulic gradient on flow velocity. This term is independent of the viscous properties of the fluid, and expresses the dependence of the pressure gradient on the square of the flow rate thorough a parameter β, the so-called Forchheimer coefficient. As an alternative, third-order polynomial laws have also been proposed (Forchheimer 1930; Mei and Auriault 1991), as well as other equations of lower order, with a fractional exponent typically ranging between one and two (Skjetne and Auriault 1999).

If non-Newtonian fluids are considered, the usual formulation of the Darcy law can be applied in the low flow regime, provided that all non-Newtonian effects are lumped together into a proper viscosity parameter, called "porous medium viscosity" (Sorbie 1991; Bird et al. 1977). It is a function of both porous medium characteristics and "bulk" viscosity, namely the viscosity of the fluid when not affected by the presence of any liquid-solid interface (Pearson and Tardy 2002; Lopez et al. 2003; Sorbie et al. 1989). Consequently, the macroscale description of the dependence of pressure drops on flow rate requires the knowledge of the bulk rheological properties of the fluid, of the permeability of the porous medium, and of an additional parameter α, called shift factor, which expresses the relationship between bulk and porous medium viscosities. The validity of this approach was demonstrated by several authors, using network modelling (Sorbie et al. 1989; Perrin et al. 2006; Lopez et al. 2003; Pearson and Tardy 2002) or from the up-scaling of the volume-averaged equation of motion (Hayes et al. 1996; Liu and Masliyah 1999).

When the flow rates are limited, the extended Darcy law for non-Newtonian fluid is thus sufficient for predicting the pressure drop. However, in practical applications higher Reynolds numbers are often encountered (Rashidi et al. 2011; Shenoy 1993) and, at this regime, an apparent increase of viscosity has been evidenced by several authors (Zhang et al. 2011; Delshad et al. 2008). This phenomenon was often attributed to a "shear thickening" behavior, arising from extensional flow of the polymeric solutions (Seright et al. 2010; Sochi 2009; Perrin et al. 2006), but Forchheimer-like phenomena cannot be excluded. A

rigorous extension of Darcy-Forchheimer law for non-Newtonian fluids, via volume-averaging of the micro-scale momentum equation, was presented for power law fluids (Hayes et al. 1996). Also, a volume-averaging approach was adopted by Liu and Masliyah (1999), who derived a generalized macroscale flow equation, and validated it against the results of pore-network flow simulations for the Cross fluid. An alternative strategy for the validation of the model is an heuristic verification of the macroscopic Darcy-Forchheimer law, against experimental pressure drop data (Macini et al. 2011). However, if this is possible when studying gas flow, when dealing with viscous fluids, pressure drops and flow rates in the inertial region may be very high, and difficult to be well controlled in laboratory-scale experiments. A viable alternative is the use of micro-scale flow simulations in reconstructed geometries, which is the approach adopted in this work.

The two most used approaches for the simulation of microscale flow are pore-network and realistic pore-scale models. In pore-network models, a portion of the porous medium is represented by a set of pores with simplified geometry (typically, spheres or spheroids) connected by a network of cylinders, where the fluid flows, and the variables (fluid velocity, pressure, or solute concentration) are solved providing an averaged value at each pore (Vogel 2000; Piri and Blunt 2005; Joekar-Niasar et al. 2010; Raoof et al. 2010; Blunt 2001; Balhoff and Thompson 2006). Alternative approaches, based for example on the solution of the Boltzmann equation, such as the particle-based Lattice-Boltzmann method (Ghassemi and Pak 2011; Zhang et al. 2000) can be used to simulate the flow. Conversely, in realistic pore-scale models an accurate reconstruction of the pore geometry is adopted, and the full Navier-Stokes and continuity equations are solved numerically over the whole pore space, thus resulting in much higher computational costs, but providing a complete description of the pressure (or velocity, or concentration) field. Different discretization techniques are used, namely standard finite volume (Bensaid et al. 2009; Bensaid et al. 2010; Ovaysi and Piri 2011), finite difference (Mostaghimi and Mahani 2010) and finite element (Narsilio et al. 2009; Rolle et al. 2012) methods, as well as hybrid ones (Zaretskiy et al. 2010). Usually, the computational grid representing the pore-scale micro-model is obtained from regular geometrical patterns, from digitalization of images of sections and polished surfaces of packed porous media

(Koplik et al. 1984; Philippi and Souza 1995; Liang et al. 1998), or from micro-computed tomography (Hazlett 1995; Narsilio et al. 2009).

In this work, an extended formulation of the Darcy-Forchheimer law for shear-thinning fluids is proposed and validated by using micro-scale flow simulations. Four different model domains, characterized by different value of porosity and specific surface area were considered, in the typical range of natural porous media in aquifer systems. Flow simulations were performed on all geometries by using the same non-Newtonian fluids (modeled by the shear thinning Cross, Ellis and Carreau fluids), to explore the impact of different pore geometries on the macroscopic average pressure drop and effective porosity. The micro-scale simulations are performed solving the Navier-Stokes and continuity equations for different two-dimensional (2D) porous media. A 2D geometry was assumed representative of single-phase three-dimensional (3D) flow, as demonstrated in the work of Chatzis and Dullien (1977). First the method is assessed for Newtonian fluids by considering a wide range of operating conditions and viscosity values (ranging from 10^{-3} to 10 Pa s). The results of the micro-scale flow simulations are analyzed in terms of "macroscale" pressure drop between the inlet and outlet of the model domain as a function of flow rate, and the permeability and Forchheimer inertial coefficient are determined via least-square fitting of the pressure data with the Darcy-Forchheimer law. Subsequently, the validity of the extended Darcy-Forchheimer law is shown for three shear-thinning models, namely the Cross (Cross 1965), Ellis (Reiner 1960) and Carreau (Carreau 1972) models. For all fluids, a broad range of flow rates was explored, both in the low flow and inertial flow regimes.

Governing equations

A linear relationship between pressure drop and specific discharge (or superficial velocity / flow rate) is assumed when describing creeping and laminar flow of a single Newtonian fluid through a fully saturated porous medium. The momentum conservation equation takes then the form of the Darcy law (Darcy 1856), that, neglecting gravity, for one-dimensional flows along the *x*-direction reads as follows:

$$\frac{\partial p}{\partial x} = \frac{\mu}{K} q \,, \tag{1}$$

where p is the pressure of the fluid [M L^{-1} T^{-2}], q is the specific discharge of the fluid [L T^{-1}], K is the permeability coefficient [L^2], μ is the fluid viscosity [M L^{-1} T^{-1}], ρ is the fluid density [M L^{-3}] and gravity is neglected here.

For Reynolds numbers in the order of one or higher a purely linear relationship between pressure drop and flow rate can no longer be assumed (Sethi 2011; Tek 1957; Dybbs and Edwards 1984). Forchheimer (Forchheimer 1901) proposed an empirical non-linear formulation by including a quadratic term to the Darcy law:

$$\frac{\partial p}{\partial x} = \frac{\mu}{K} q + \beta \rho\, q|q| \,, \tag{2}$$

where β is the so-called inertial flow parameter [L^{-1}]. Equation (2) reduces to (1) for small q.

The permeability K is a macroscopic parameter describing up-scaled effects of the microscopic configuration of the void space in the porous medium (Bear 1988) and therefore is assumed independent on fluid properties. Also the parameter β of the Darcy-Forchheimer equation depends only on the microstructure of the porous medium, as demonstrated by Hayes et al. (1996).

As an alternative, semi-empirical relationships relating the macro-scale parameters of the porous medium, K and β, to other macroscopic properties of a porous medium, such as the average porosity, ε, and the specific surface area, a, have been proposed by different authors (Bird et al. 2002). The well known Ergun equation was originally derived for a packed bed of homogeneous spheres, fully saturated in a Newtonian fluid, starting from the analogy between flow through pores and pipes, by combining the Blake-Kozeny equation (Blake 1922) valid for laminar flow, and the Burke-Plummer equation (Burke and Plummer 1928) developed for non-linear flow. For bed grains of a generic shape, following the methodology of Ergun, it is possible re-write the Ergun equation and to re-arrange it for the direct comparison to the Darcy-Forchheimer's equation. The Ergun equation takes then the form:

$$\frac{\partial p}{\partial x} = \frac{25}{6} \frac{a^2}{\varepsilon^3} \mu\, q + \frac{7}{24} \frac{a}{\varepsilon^3} \rho\, q|q| \,, \tag{3}$$

where a is the specific surface of the soil grains [L^{-1}]. By comparing Eqs. (2) and (3) it is possible to relate the permeability coefficient K and the inertial flow parameter β to the parameters a and ε of the Ergun equation:

$$K = \frac{6}{25} \frac{\varepsilon^3}{a^2} , \qquad\qquad (4.a)$$

$$\beta = \frac{7}{24} \frac{a}{\varepsilon^3} . \qquad\qquad (4.b)$$

The resulting formulation for K is very similar to the semi-empirical Carman-Kozeny equation (Kozeny 1927; Carman 1937):

$$K = \frac{1}{5} \frac{\varepsilon^3}{a^2} . \qquad\qquad (5)$$

The dependence of the flow inertial parameter β on porous medium properties was investigated by several authors, especially in the field of reservoir engineering, using approximated models for the pore-space configuration, or deriving empirical or semi-empirical relationships from experimental data, (Geertsma 1974; Kalaydjian et al. 1996; Macini et al. 2011).

As far as the rheological properties of the investigated fluid are concerned, for Newtonian fluids the dependence of the shear stress τ on the shear rate $\dot{\gamma}$ is expressed by a linear relationship, $\tau = \mu \dot{\gamma}$, where the (constant) coefficient μ is the fluid viscosity [M L^{-1} T^{-1}]. However, when dealing with non-Newtonian fluids, this simple relationship fails, and more complex formulations are to be considered, depending on the rheological model, and the viscosity (often referred to as apparent viscosity) is a function of the shear rate itself, $\tau = \mu(\dot{\gamma})\dot{\gamma}$. The second column of Table 1 reports four rheological models used for the description of shear-thinning fluids, namely the power-law, Cross, Ellis and Carreau models.

When modelling the laminar flow of non-Newtonian fluids in porous media, also the Darcy law has to be modified accordingly. Under steady-state flow conditions, the so-called generalized Newtonian fluid model can be adopted (Bird et al. 2002; Bird et al. 1977). The model relies on the hypothesis that the same equations used for Newtonian flow can be applied also to non-Newtonian fluids, provided that the constant viscosity μ is replaced in the equations by the "porous medium viscosity", μ_m, which depends on both porous medium characteristics and fluid

properties (Sorbie et al. 1989; Pearson and Tardy 2002; Lopez et al. 2003; Bird et al. 1977).

As bulk viscosity is a function of the shear rate, also the porous medium viscosity is related to the so-called "porous medium shear rate" ($\dot{\gamma}_m$), defined as the average shear rate that the fluid experiences while flowing through the pores (Bird et al. 2002; Taylor and Nasr-El-Din 1998). The modified Darcy law for non-Newtonian fluid is therefore:

$$\frac{\partial p}{\partial x} = \frac{\mu_m(\dot{\gamma}_m)}{K} q ,$$

(6)

where $\dot{\gamma}_m$ can be estimated dividing the absolute value of the specific discharge $|q|$ by a characteristic microscopic length of the porous medium (i.e., $\sqrt{K\varepsilon}$) as indicated by (Perrin et al. 2006; Sorbie 1991) resulting in:

$$\dot{\gamma}_m = \alpha \frac{|q|}{\sqrt{K\varepsilon}} .$$

(7)

Experimental tests confirmed that rheograms (i.e., plots of apparent viscosity as a function of shear rate) of the bulk fluid and those derived from injection in one-dimensional porous medium are shifted by a constant value α, often referred to as shift factor. From a physical point of view, the shift factor contains information about the effects of the pore-scale geometry of the porous medium on the local fluid velocity and velocity gradients and, as a consequence, on the overall apparent viscosity obtained in the up-scaling from the pore-scale microscopic domain to the macroscopic (continuous) medium. This is in agreement with experimental shifts observed between experimental rheograms in the bulk and in the porous media characterized by different degrees of complexity. Typical values of α, determined comparing experimental data of viscosity versus flow rate in the bulk and in porous media, are reported to be usually in the range from one to 15 (Lopez et al. 2003). Experiments conducted in homogeneous, ordered and well sorted porous media evidenced values of the shift factor α typically close to one, while those conducted in porous media characterized by increasing complexity and inhomogeneity resulted in higher α values (Sorbie et al. 1989). For power-law fluids, it has been demonstrated (Sorbie et al. 1989) that, while flowing through a capillary, the shift factor is also affected by the rheological properties of the fluid. Also, similar results were obtained from flow simulations in network

models (Pearson and Tardy 2002), which evidenced the concurrent dependence of α on the power-law exponent and the tortuosity of the network. Consequently, unlike K and β, the shift factor α is not an intrinsic property of the porous medium, and consequently it is to be determined for each fluid and porous medium from laboratory flow tests or from pore-level flow simulations, which is the approach followed in this work.

Increasing the Reynolds number, also non-Newtonian fluids give rise to additional contributions to the pressure drop, characterized by a non-linear dependence on the specific discharge. They can be modelled by adding the Forchheimer term to the extended Darcy law reported in Eq. (6). Following the literature, it is possible to hypothesize that the non-linearities are due to inertial phenomena, and consequently do not depend on the viscous properties of the fluid (Hayes et al. 1996). The pressure drop can therefore be quantified with the modified Darcy-Forchheimer equation:

$$\frac{\partial p}{\partial x} = \frac{\mu_m(\dot{\gamma}_m)}{K} q + \beta \rho q |q| . \tag{8}$$

The purpose of this work is to verify the validity of this law also for several non-Newtonian fluids (such as the other ones reported in Table 1). The validity of the approach is discussed by proving that Eq. (8) correctly models pore-scale simulated data of pressure drops versus discharge rate.

The analysis can be carried out by making use of the concept of equivalent viscosity, μ_{eq}. This quantity is defined as the expression that must replace the viscosity in the Darcy law in order to result in the same pressure drop predicted by the Darcy-Forchheimer equation:

$$\mu_{eq} = \frac{\partial p/\partial x}{q} K , \tag{9}$$

where $\partial p/\partial x$ is the measured pressure drop and K is the Darcyan permeability (i.e., the permeability value obtained at very low discharge). The Darcy-Forchheimer equation can therefore be re-written in a form similar to the classic Darcy law, with only one term expressing the (fictitious) linear dependence on the flow rate.

Comparison of Eq. (2) with Eq. (9) results in the following definition for the equivalent viscosity:

$$\mu_{eq} = \mu + \beta \rho K |q|, \tag{10}$$

valid in the case of Newtonian fluids. As evident from Eq. (10), the increase in the pressure drops due to the non-linear term can be interpreted as a "fictitious" increase of viscosity, generated by inertial phenomena.

Similarly to Newtonian fluids, also in the case of shear-thinning fluids the Darcy-Forchheimer equation can be re-arranged introducing the equivalent viscosity, resulting in the following expression:

$$\mu_{eq}\left(\dot{\gamma}_m\right) = \mu_m\left(\dot{\gamma}_m\right) + \beta \rho K |q|. \tag{11}$$

Closer observation of Eq. (11) shows that the dependence of μ_{eq} versus the flow rate highlights the presence of two terms. The first one represents the porous medium viscosity, which dominates at low flow rates and depends on the fluid rheological behaviour and on the characteristics of the porous medium. The second term represents instead the additional, "fictitious", non-linear viscosity generated by inertial phenomena, which is not affected by the rheological properties of the fluid, and dominates at high flow rates.

If the Cross model for the shear-thinning fluids is considered (see second row of Table 1), the equivalent viscosity μ_{eq} is obtained from Eq. (11), resulting in the following expression:

$$\mu_{eq} = \mu_\infty + \frac{\mu_0 - \mu_\infty}{\left[1 + \left(\frac{\lambda \alpha}{\sqrt{K\varepsilon}}\right)^{\chi} |q|^{\chi}\right]} + \beta \rho K |q| , \tag{12}$$

where the shear rate $\dot{\gamma}_m$ was replaced by the porous medium shear rate defined in Eq. (7).

As evident from Eq. (12) the equivalent viscosity is in this case due to three contributions: (i) a term independent of fluid velocity (and shear rate) due to the second Newtonian plateau, μ_∞; (ii) a non-linear term, that includes all non-Newtonian effects and depends on fluid properties (shear-thinning model parameters), porous medium properties (K, ε and α) and flow rate; (iii) the Forchheimer additional term, which is here supposed not to be affected by the rheological properties of the fluid. Similar considerations can be inferred for the Ellis and Carreau viscosity models, as shown in Table 1. When considering

experimental data of equivalent viscosity, the contribute of each term in Eq. (12) to the overall μ_{eq} can be clearly identified and separated: the first term is a constant value, and can be derived from the bulk rheological properties of the fluid (i.e. μ_∞ is a known parameter); the second term dominates at low shear rates (or specific discharges), i.e. in the low-rate flow regime, and can be consequently quantitatively determined if considering the viscosity data obtained for Reynolds numbers smaller than one; the third term, i.e. the Forchheimer additional viscosity, dominates in the inertial flow regime, and consequently can be calculated when the other two are known.

The validity of the extended Darcy-Forchheimer law for non-Newtonian fluids is assessed in this work for shear thinning rheological models by using the pore-scale simulations described in the next section.

Pore-scale flow simulations

The model domains used in pore-scale simulations were obtained from scanning electron microscopy (SEM) images of natural unpacked sand grains, that were then digitalized and processed in order to extract the contour of the grains. The contour of each grain was then processed as an independent (closed) object: grains were located in the model domain in order to reach the desired value of porosity (). The region corresponding to the pore space of the medium was then discretized using GAMBIT® 2.4.6. The computational grids were obtained with an iterative process of grid refinement, up to a final number of quadrilateral cells ranging of 3 to 6 $\times 10^5$. In fact, further refinements did not result in significantly different predictions for the pressure drops, showing that with this discretization the momentum boundary layer around the grains is fully resolved.

Four model domains (corresponding to four different computational grids) were used in this work, each characterized by different mean grain size and porosity. The porosity (ε) varied between 0.4 and 0.5 whereas the mean grain size varied in the range between 0.5 and 1 mm, resulting in specific surface areas ranging from 6×10^3 to 1×10^4 m^{-1}. A summary is reported in Table 2 along with the labels (grid 1, 2, 3, 4) used in the following to identify the different grids. Each domain represents a small portion of porous medium (3 mm to 1 cm in length). The values

of grain size and porosity were selected as representative of typical porous media encountered in groundwater engineering, corresponding to shallow permeable aquifer systems. Other applications (e.g. petroleum engineering or filtration towers in industrial processes) would require to broaden the explored range of the parameters.

Numerical flow simulations for Newtonian and non-Newtonian fluids in the described two-dimensional domains were performed by solving the full continuity and Navier-Stokes equations by using the commercial computational fluid dynamics (CFD) code ANSYS Fluent 13.0 (based on a finite-volume discretization). A CFD approach was here used for describing the steady-state single-phase flow of Newtonian and non-Newtonian fluids through the pores by solving the continuity and Navier-Stokes equations, that written with the Einstein notation for an incompressible fluid read as follows:

$$\begin{cases} \dfrac{\partial v_i}{\partial x_i} = 0 \\ \rho \left(\dfrac{\partial v_i}{\partial t} + v_j \dfrac{\partial v_i}{\partial x_j} \right) = - \dfrac{\partial p}{\partial x_i} + \dfrac{\partial \tau_{ij}}{\partial x_j} \end{cases} \qquad (13)$$

where v_i is the ith component of the fluid velocity in the pores [L T^{-1}], and τ_{ij} is the shear stress tensor [M L^{-1} T^{-2}].

In the case of Newtonian fluids τ_{ij} is written as follows:

$$\tau_{ij} = \mu \left(\dfrac{\partial v_i}{\partial x_j} + \dfrac{\partial v_j}{\partial x_i} \right) = 2 \mu E_{ij} \qquad (14)$$

where E_{ij} is the rate-of-strain tensor [T^{-1}].

For all grids, laminar single-phase flow simulations were first run for Newtonian fluids with different values of viscosity (10^{-3} to 10 Pa s) and specific discharge (approximately $5 \times 10^{-7} - 5$ m/s). The corresponding average Reynolds numbers for the porous media vary in the range 10^{-7} (lowest flow rate, highest viscosity) to 10^3 (highest flow rate, lowest viscosity). Then non-Newtonian fluids, described by the Cross, Ellis and Carreau rheological models were simulated by replacing the constant Newtonian viscosity with the apparent viscosity calculated from the equations reported in Table 1. In this equation the shear rate is calculated as the second invariant of the velocity gradient tensor. The values adopted for the model

parameters (μ_∞, μ_0, λ, χ for Cross and Carreau models, μ_0, λ, χ for Ellis model) were obtained from inverse fitting of experimental rheological characterization of shear thinning fluids used in reservoir and environmental applications. In particular, the viscosity curve of a xanthan gum solution (3 g/l) was used for the rheological models of Cross and Ellis, while guar gum (5 g/l) was used as reference for the Carreau model. The numerical values of the curve parameters are reported in Table 3 whereas the corresponding viscosity curves are reported in .

For all fluids a density of 998.2 kg/m^3 was used. The boundary conditions applied for the governing equations were of constant mass flow inlet in the upper edge, where the fluid enters the domain, and of outflow in the lower edge, where the fluid exits the domain. Symmetric boundary conditions were instead selected for the two lateral edges. This implies that the fluid is moving parallel to the lateral edges, as no (convective or diffusive) flux is allowed in the direction normal to the later edges. This choice was selected among the other options (e.g., period boundary conditions) as the least invasive and arbitrary, and as the most sensible and realistic for pore-scale similations. The SIMPLE algorithm was used for the pressure-velocity coupling.

For each simulation, the pressure integral drop $\Delta p / L \approx \partial p / \partial x$ between the entrance (top) and exit (bottom) of the computational domain was evaluated and analyzed by using the Darcy-Forchheimer equation, as discussed below.

Results and discussion

The macroscale parameters K and β for each computational grid were first calculated from the mean macro-scale properties, namely porosity and specific surface area, from Eqs. (4), obtained in turn from the Ergun law (Table 2). As a general rule, when decreasing porosity, the permeability decreases too, whereas a reduction in the specific surface area causes an increase in permeability. These two sets of values of K and β can be then compared to those obtained via least-square fitting of pressure drop results from microscale flow simulations.

Steady-state single-phase Navier-Stokes flow simulations for Newtonian fluids were run on all four computational grids, for a range of viscosity (10^{-3} to 10 Pa s). A typical example for the contour plot of fluid velocity magnitude is shown in .

Comparison of contour plots from simulations carried out varying the inlet flow velocity (i.e., discharge or superficial velocity) and the fluid viscosity, highlights the complex interaction within this confined network of pores. From each simulation, pressure drop and average flow parameters were calculated. The parameters K and β for each computational grid were both obtained via least-square fitting of data. The fitted parameters corresponding to Newtonian fluids are detailed in the fourth column of Table 4. The quality of the fitting can be evaluated by plotting the results in terms of the normalized pressure drops $\left(\Delta p/L\right)\big/\rho\,q^2$ versus the normalized superficial velocity $\left(\rho\,|q|\right)\big/\mu$, following the convention usually employed for the representation of the Ergun law (Bird et al. 2002).

Two examples are reported in and , that show the data collected for Newtonian fluids of different constant viscosities, flowing under different flow rates for Grids 3 and 4, reported in terms of these normalized quantities in log-log plots. As it is seen, all the different data points collapse into one single master curve, that accurately reproduces them, proving the excellent quality of the fitting. Moreover, this representation also allows an easy identification of the parameters: in the low flow regime, the normalized pressure drop $\left(\Delta p/L\right)\big/\rho\,q^2$ is follows a straight line in a logarithmic plot. On the contrary, in the inertial flow regime, $\left(\Delta p/L\right)\big/\rho\,q^2$ reaches an asymptote, corresponding to the Forchheimer coefficient β.

In the figures the data points from the micro-scale flow simulations are not only compared with the fitted Darcy-Forchheimer law, but also with the Ergun law and the Darcy law. The Darcy law accurately models the data points for low and intermediate flow rates, up to Reynolds number approximately equal to ten. A further increase in the flow rate evidences the departure of the pore-scale pressure drop data from the straight Darcy line, and the trend is correctly captured by the Darcy-Forchheimer law. The Ergun law describes fairly well the first part of the curve but then predicts a different asymptotic value. This is reflected by the data reported in Table 4. When comparing K and β predicted by the Ergun law (third column) and fitted with the Darcy-Forchheimer law (fourth column), it is evident that the agreement between the two sets of values is satisfactory for K (with a partial exception of Grid 1), more critical for β (for which a general

overestimation is observed for Ergun Equation). This finding suggests that, especially when exploring inertial flow, the estimation of the macro-scale parameters from macroscopic properties (i.e. porosity and specific surface area) cannot be used alone for an accurate prediction of pressure drop: flow simulations or flow tests are to be performed, and also other parameters, such as tortuosity, should be taken into account.

Flow simulations for non-Newtonian fluids were run over a wide range of specific discharge (approximately $5 \times 10^{-7} - 5$ m/s) for all grids. The rheological models of Cross, Ellis and Carreau for guar gum and xanthan gum solutions were adopted, corresponding to the rheologic parameters reported in Table 3 and the rheogram plotted in . Simulation results, in terms of steady-state pressure drop between entrance and exit of the model domain, were then analyzed against flow rate to verfy the hypothesis that the Darcy-Forchheimer equation can be applied also to shear thinning fluids and that the quadratic Forchheimer term is independent of the rheological properties of the fluid. The permeability was assumed independent of the fluid properties, while the inertial coefficient β and the shift factor α were least-squared fitted, to prove the independence of β on fluid properties.

Contrary to Newtonian fluids, in the case of shear-thinning fluids it is more convenient to analyze pressure data expressed in the form of the generalized Darcy model reported in Eq. (9), and referring to the concept of equivalent viscosity μ_{eq}. For each micro-scale flow simulation, which provides a pressure drop $\Delta p / L$ between inlet and outlet of the domain, a value of μ_{eq} can be calculated as $K / q \cdot \Delta p / L$, following Eq. (11). When μ_{eq} is reported as a function of the specific discharge, different trends are found for each fluid model and each grid (an example is shown in for the Cross fluid). Conversely, μ_{eq} can be also reported as a function of the porous medium shear rate, $\dot{\gamma}_m$, which was defined in Eq. (7), in order to better highlight the impact of inertial flow on pressure drops. In this case, all data in the low flow regime collapse onto the rheological curve of $\mu_m(\dot{\gamma}_m)$ (see , again for the Cross model results). Conversely, data in the inertial flow regime, usually for shear rates in the order of 10^4 s^{-1}, diverge from the bulk rheological curve, and are aligned along a straight line (in the log-log graph) which is specific of the porous medium.

A similar behaviour was observed in a number of empirical data of pressure drops due to the flow of polymeric solutions at high flow rates in porous columns (Delshad et al. 2008; Zhang et al. 2011). For these data, the deviation from the rheological bulk curve at high flow rates (called shear thickening behaviour) was attributed to the extensional flow of the polymeric solutions: above a critical flow rate, polymer chains flowing through the pores are subject to periodical elongation and contraction, due to rapid changes in flow directions when moving along the tortuous paths of the flow lines. Changes in direction take place with a frequency higher than the relaxation time, and the effect is then the observed apparent increase in viscosity. In the micro-scale simulations presented in our work the elastic properties of the shear thinning fluid were not included, and consequently the deviation from the rheological bulk curve observed in all plots cannot be attributed to elongational effects. It is then possible to hypothesize that the experimental evidence of "shear thickening" in porous media can be partly attributed to the elastic properties of the real fluid, but also, under some circumstances, to the inertial effects modelled by the quadratic term of the Darcy-Forchheimer fluid.

When non-Newtonian flow is considered, three macroscale parameters are required for the prediction of pressure drops, namely the permeability K, the inertial coefficient β, and the shift factor α. Following the procedure adopted for Newtonian fluids, also for the shear thinning fluids the pressure drop data from pore-scale flow simulations were fitted against the Darcy-Forchheimer law. The permeability was here assumed independent of fluid properties: the K values from the least-square fitting of Newtonian flow data, previously discussed, were adopted in the non-Newtonian flow analysis. Consequently, only β and α were determined, for each grid and rheological model (Table 4). The least-squares fitted values of the shift factor α fall in the range 1.5 to 5.5, which is consistent with the values expected from the literature (Lopez et al. 2003). The resulting values of β were compared with those obtained for Newtonian fluids (). For all grids, the values of inertial coefficient β obtained for the non-Newtonian flow simulations are in agreement among them, and with the values obtained for Newtonian fluids, and no evident influence of the fluid rheology is observed. This

finding supports the initial hypothesis that the inertial coefficient β is independent of fluid properties also in case of shear thinning fluids.

 to show the results of μ_{eq} versus $\dot{\gamma}_m$ for the three investigated shear-thinning models. The values of equivalent viscosity calculated from micro-scale flow simulations (symbols) are compared with the least-squares fitted curves obtained by using Eq. (11). The contribution of the two components, namely the porous medium viscosity $\mu_m(\dot{\gamma}_m)$ and the inertial term $\beta \rho K |q|$ are also highlighted (solid and dotted lines, respectively). For all three rheological models the figures show that, in the low flow regime, shear thinning effects dominate, and the data points of μ_{eq} for all grids are correctly modelled by the fluid rheological curve $\mu_m(\dot{\gamma}_m)$ (solid lines in to). Conversely, when increasing flow rate, the additional contribution to the pressure drops due to inertial phenomena increases, and the "fictitious" viscosity term $\beta \rho K |q|$ dominates (dashed lines). For all grids, the term becomes important for shear rates in the order of 10^4 s^{-1}, and Reynolds numbers in the order of one to seven. The additional "non-linear" viscosity term differs from one grid to another (it depends on macroscopic parameters K and β), but is independent of the rheological model. Proof of this is shown in , where the data corresponding to Grid 3 for all rheological models are reported. As it is evident here, μ_{eq} depends only on fluid viscosity at low shear rate, while increasing shear rate all data collapse into one single straight line. The increase of equivalent viscosity at high Reynolds numbers is in agreement with previously reported experimental data of pressure drops in column flow tests for a shear thinning fluids (Perrin et al. 2006).

This final remark strongly suggests that the Darcy-Forchheimer law can be extended to non-Newtonian fluids, represented by models other than the simple power law, such as Cross, Ellis and Carreau models. This has important practical applications. The Darcy-Forchheimer law can be directly applied to the design and the optimization of those processes involving flows of non-Newtonian fluids in porous media, including large-scale simulation of flow in porous media, where the details of the porous structure cannot be fully described but are to be modelled.

Conclusions and practical implications

Four geometries along with the corresponding computational grids were constructed from real images of sand grains. First, Newtonian flow simulations at the micro-scale were run and results used for grid validation; the determination of porous medium permeability K and inertial coefficient β produced results consistent with the Ergun law. The analysis of the simulation results in terms of pressure drops over the entire domain as a function of flow rate showed that they can be accurately modeled by the Darcy-Forchheimer law over a wide range of flow rates.

In a second step, micro-scale flow simulations were run for non-Newtonian fluids, using three different rheological models for shear-thinning fluids (Cross, Ellis and Carreau models). The analysis of the pressure drops obtained from non-Newtonian flow simulations confirmed the applicability of the Darcy-Forchheimer law to non-Newtonian fluids other than power law fluids, for which the law validity was previously demonstrated. This finding opens perspectives for a wide range of applications, where the pressure gradients generated by non-Newtonian flow at high velocity are to be predicted.

In case of Newtonian flow the porous medium can be fully described by two macroscopic parameters, namely permeability K and inertial coefficient β. On the contrary, inverse modeling of pressure drops with the Darcy-Forchheimer law evidenced that, in case of non-Newtonian flow, an additional parameter is required, represented by the shift factor α, which depends on the properties of both porous medium and fluid. Therefore, in case of non-Newtonian fluid flow, the estimation of the pressure drops requires three macroscale parameters. From a practical point of view, permeability and shift factor can be easily determined in the laboratory from column flow tests, performed using the non-Newtonian fluid. Conversely, the determination of the inertial coefficient β from column tests with a highly viscous fluid may be difficult in some cases, due to the high pressures and flow rates involved. A possible protocol for the determination of the three parameters could instead couple gas and fluid flow tests: gas flow tests, which involve pressure drops easy to be controlled in the laboratory, can be performed

for the determination of permeability K and inertial coefficient β, exploring both linear and non-linear flow regimes. Flow tests involving the non-Newtonian fluids, limited to the low flow regime, can be then performed for the determination of the shift factor α. As an alternative, if the pore-level structure of the medium is known sufficiently in detail (e.g. from 3D micro-tomography imaging), all three parameters can be determined from 2D or 3D pore-scale flow simulations, following the approach which was adopted in this work. This method has the advantage of allowing exploring a (potentially) unlimited range of fluids (both Newtonian and non-Newtonian), as well as a wide range of flow rate and pressure, which may be in turn prohibitive in laboratory tests.

Future steps of this work include the extension of this two-dimensional analysis to the problem of particle transport and deposition (on grains) using both Eulerian and Lagrangian approaches for the particle-phase. The extension of the present analysis (limited to the flow of Newtonian and non-Newtonian fluids without particles) to three-dimensional porous media will also be investigated in the near future.

References

Auradou, H., Boschan, A., Chertcoff, R., Gabbanelli, S., Hulin, J.P., Ippolito, I.: Enhancement of velocity contrasts by shear-thinning solutions flowing in a rough fracture. J. Non-Newton. Fluid Mech. **153**(1), 53-61 (2008)

Balhoff, M.T., Thompson, K.E.: A macroscopic model for shear-thinning flow in packed beds based on network modeling. Chem. Eng. Sci. **61**(2), 698-719 (2006)

Battiato, I., Tartakovsky, D.M., Tartakovsky, A.M., Scheibe, T.D.: Hybrid models of reactive transport in porous and fractured media. Advances in Water Resources 34(9), 1140-1150 (2011)

Bear, J.: Dynamics of fluids in porous media. Dover books on physics and chemistry. Dover, New York (1988)

Bensaid, S., Marchisio, D.L., Fino, D.: Numerical simulation of soot filtration and combustion within diesel particulate filters. Chem. Eng. Sci. **65**(1), 357-363 (2010)

Bensaid, S., Marchisio, D.L., Fino, D., Saracco, G., Specchia, V.: Modelling of diesel particulate filtration in wall-flow traps. Chem. Eng. J. **154**(1-3), 211-218 (2009)

Bird, R.B., Armstrong, R.C., Hassager, O.: Dynamics of polymeric liquids. Volume 1. Fluid mechanics. John Wiley and Sons Inc., New York - NY (1977)

Bird, R.B., Stewart, W.E., Lightfoot, E.N.: Transport phenomena, 2nd, Wiley international ed. J. Wiley, New York (2002)

Blake, F.C.: The resistance of packing to fluid flow. Trans. Am. Inst. Chem. Eng. **14**, 415-421 (1922)

Blunt, M.J.: Flow in porous media - Pore-network models and multiphase flow. Current Opinion in J. Colloid Interface Sci. **6**(3), 197-207 (2001)

Burke, S.P., Plummer, W.B.: Gas Flow through Packed Columns1. nd. & Eng. Chem. **20**(11), 1196-1200 (1928). doi:10.1021/ie50227a025

Carman, P.C.: Fluid flow through granular beds. Chem. Eng. Res. Des. **75**(Supplement 1), S32-S48 (1937)

Carreau, P.J.: Rheological equations from molecular network theories. Trans. Soc. Rheol. **16**(1), 99-127 (1972)

Chatzis, I., Dullien, F.A.L.: Modelling pore structure by 2-D and 3-D networks with application to sandstones . J. Can. Petrol. Technol. **16**(1), 97-108 (1977)

Ciriello, V., Di Federico, V.: Similarity solutions for flow of non-Newtonian fluids in porous media revisited under parameter uncertainty. Adv. Water Res. **43**(0), 38-51 (2012)

Cross, M.M.: Rheology of non-Newtonian fluids: A new flow equation for pseudoplastic systems. J. Colloid Sci. **20**(5), 417-437 (1965)

Dalla Vecchia, E., Luna, M., Sethi, R.: Transport in Porous Media of Highly Concentrated Iron Micro- and Nanoparticles in the Presence of Xanthan Gum. Environ. Sci. Tech. **43**(23), 8942-8947 (2009). doi:Doi 10.1021/Es901897d

Darcy, H.: Les fontaines publiques de la ville de Dijon. Dalmont, Paris (1856)

Delshad, M., Kim, D.H., Magbagbeola, O.A., Huh, C., Pope, G.A., Tarahhom, F.: Mechanistic interpretation and utilization of viscoelastic behavior of polymer solutions for improved polymer-flood efficiency. In: SPE/DOE Symposium on Improved Oil Recovery, 2008, pp. 1051-1065

Dybbs, A., Edwards, R.V.: A new look at porous media fluid mechanics - Darcy to turbolent Foundamentals of Transport Phenomena in Porous media. J. Bear and M.Y. Corapcioglu (eds.), Martinus Nijhoff, Dordrecht, 199-256 (1984)

Forchheimer, P.: Wasserbewegung durch Boden. Z. Ver. Deutsch. Ing. **45**, 1782-1788 (1901)

Forchheimer, P.: Hydraulik, 3 Aufl., ed. B. G. Teubner, Leipzig, Berlin, (1930)

Geertsma, J.: Estimating the coefficient of inertial resistance in fluid flow through porous media. Soc Pet Eng AIME J **14**(5), 445-450 (1974)

Ghassemi, A., Pak, A.: Pore scale study of permeability and tortuosity for flow through particulate media using Lattice Boltzmann method. Int. J. Num. Anal. Meth. Geomech. **35**(8), 886-901 (2011)

Hassanizadeh, S.M., Gray, W.G.: High-Velocity Flow in Porous-Media. Transp. Porous Media **2**(6), 521-531 (1987)

Hayes, R.E., Afacan, A., Boulanger, B., Shenoy, A.V.: Modelling the flow of power law fluids in a packed bed using a volume-averaged equation of motion. Transp. Porous Media **23**(2), 175-196 (1996). doi:10.1007/bf00178125

Hazlett, R.D.: Simulation of capillary-dominated displacements in microtomographic images of reservoir rocks. Transp. Porous Media **20**(1-2), 21-35 (1995)

Innocentini, M.D.M., Salvini, V.R., Pandolfelli, V.C., Coury, J.R.: Assessment of Forchheimer's equation to predict the permeability of ceramic foams. J. Am. Ceram. Soc. **82**(7), 1945-1948 (1999)

Joekar-Niasar, V., Prodanović, M., Wildenschild, D., Hassanizadeh, S.M.: Network model investigation of interfacial area, capillary pressure and saturation relationships in granular porous media. W Water Res. Res. **46**(6) (2010)

Kalaydjian, F.J.M., Bourbiaux, B.J., Lombard, J.M.: Predicting gas-condensate reservoir performance: How flow parameters are altered when approaching production wells. In: Annual Technical Conference and Exhibition. Part Delta, Denver, CO, USA 1996, pp. 355-369

Koplik, J., Lin, C., Vermette, M.: Conductivity and permeability from microgeometry. J. Appl. Phys. **56**(11), 3127-3131 (1984)

Kozeny, J.: Uber Kapillare Leitung des Wasser im Boden. Sitzungsberichte der Akademie der Wissenschaften Wien **136**, 106-271 (1927)

Lee, S., Ang, W.S., Elimelech, M.: Fouling of reverse osmosis membranes by hydrophilic organic matter: Implications for water reuse. Desalination **187**(1-3), 313-321 (2006)

Levy, A., Levi-Hevroni, D., Sorek, S., Ben-Dor, G.: Derivation of Forchheimer terms and their verification by application to waves propagation in porous media. Int. J. Multiph. Flow **25**(4), 683-704 (1999)

Liang, Z.R., Fernandes, C.P., Magnani, F.S., Philippi, P.C.: A reconstruction technique for three-dimensional porous media using image analysis and Fourier transforms. J. Pet. Sci. Eng. **21**(3-4), 273-283 (1998)

Liu, S., Masliyah, J.H.: On non-Newtonian fluid flow in ducts and porous media. Chem. Eng. Sci. **53**(6), 1175-1201 (1998)

Liu, S., Masliyah, J.H.: Non-linear flows in porous media. J. Non-Newton. Fluid Mech. **86**(1-2), 229-252 (1999)

Lopez, X., Valvatne, P.H., Blunt, M.J.: Predictive network modeling of single-phase non-Newtonian flow in porous media. J. Colloid Interface Sci. **264**(1), 256-265 (2003). doi:10.1016/s0021-9797(03)00310-2

Macini, P., Mesini, E., Viola, R.: Laboratory measurements of non-Darcy flow coefficients in natural and artificial unconsolidated porous media. J. Pet. Sci. Eng. **77**(3-4), 365-374 (2011)

Mei, C.C., Auriault, J.L.: The effect of weak inertia on flow through a porous medium. J. Fluid Mech. **222**, 647-664 (1991)

Mostaghimi, P., Mahani, H.: A Quantitative and Qualitative Comparison of Coarse-Grid-Generation Techniques for Modeling Fluid Displacement in Heterogeneous Porous Media. SPE Res. Eval. Eng. **13**(1), pp. 24-36 (2010). doi:10.2118/118712-pa

Muskat, M., Wyckoff, R.D.: The flow of homogeneous fluids through porous media, 1st ed. International series in physics. McGraw-Hill Book Company, inc., New York, London, (1937)

Narsilio, G.A., Buzzi, O., Fityus, S., Yun, T.S., Smith, D.W.: Upscaling of Navier–Stokes equations in porous media: Theoretical, numerical and experimental approach. Comp. Geotech. **36**(7), 1200-1206 (2009)

Ovaysi, S., Piri, M.: Pore-scale modeling of dispersion in disordered porous media. J. Contam. Hydrol. **124**(1-4), 68-81 (2011)

Pearson, J.R.A., Tardy, P.M.J.: Models for flow of non-Newtonian and complex fluids through porous media. J. Non-Newton. Fluid Mech. **102**(2), 447-473 (2002)

Perrin, C.L., Tardy, P.M.J., Sorbie, K.S., Crawshaw, J.C.: Experimental and modeling study of Newtonian and non-Newtonian fluid flow in pore network micromodels. J. Colloid Interface Sci. **295**(2), 542-550 (2006). doi:DOI 10.1016/j.jcis.2005.09.012

Philippi, P.C., Souza, H.A.: Modelling moisture distribution and isothermal transfer in a heterogeneous porous material. Int. J. Multiph. Flow **21**(4), 667-691 (1995)

Piri, M., Blunt, M.J.: Three-dimensional mixed-wet random pore-scale network modeling of two- and three-phase flow in porous media. I. Model description. Phys. Rev. E **71**(2) (2005). doi:02630110.1103/PhysRevE.71.026301

Raoof, A., Majid Hassanizadeh, S., Leijnse, A.: Upscaling transport of adsorbing solutes in porous media: Pore-network modeling. Vadose Zone J. **9**(3), 624-636 (2010)

Rashidi, M.M., Keimanesh, M., Bég, O.A., Hung, T.K.: Magnetohydrodynamic biorheological transport phenomena in a porous medium: A simulation of magnetic blood flow control and filtration. nternational J. Num. Meth. Biomed. Eng. 27(6), 805-821 (2011)

Reiner, M.: Deformation, strain, and flow; an elementary introduction to rheology, [2d ed. Interscience Publishers, New York, (1960)

Rolle, M., Hochstetler, D., Chiogna, G., Kitanidis, P.K., Grathwohl, P.: Experimental Investigation and Pore-Scale Modeling Interpretation of Compound-Specific Transverse Dispersion in Porous Media. Transp. Porous Media 93(3), 347-362 (2012)

Seright, R.S., Fan, T., Wavrik, K., Balaban, R.D.C.: New insights into polymer rheology in porous media. In: 17th SPE Improved Oil Recovery Symposium 2010, pp. 130-140

Sethi, R.: A dual-well step drawdown method for the estimation of linear and non-linear flow parameters and wellbore skin factor in confined aquifer systems. J. Hydrol. 400(1-2), 187-194 (2011)

Shenoy, A.V.: Darcy-Forchheimer natural, forced and mixed convection heat transfer in non-Newtonian power-law fluid-saturated porous media. Transp. Porous Media 11(3), 219-241 (1993)

Skjetne, E., Auriault, J.L.: High-velocity laminar and turbulent flow in porous media. Transp. Porous Media 36(2), 131-147 (1999)

Sochi, T.: Pore-scale modeling of viscoelastic flow in porous media using a Bautista–Manero fluid. Int. J. Heat Fluid Flow 30(6), 1202-1217 (2009)

Sorbie, K.S.: Polymer-improved oil recovery. Blackie ; CRC Press, Glasgow, Boca Raton, Fla. (1991)

Sorbie, K.S., Clifford, P.J., Jones, E.R.W.: The rheology of pseaudoplastic fluids in porous media using network modeling. J. Colloid Interface Sci. 130(2), 508-534 (1989)

Taylor, K.C., Nasr-El-Din, H.A.: Water-soluble hydrophobically associating polymers for improved oil recovery: A literature review. J. Pet. Sci. Eng. 19(3-4), 265-280 (1998)

Tek, M.R.: Development of a Generalized Darcy Equation. J. Pet. Tech. 9(6), 45-47 (1957)

Tosco, T., Bosch, J., Meckenstock, R.U., Sethi, R.: Transport of ferrihydrite nanoparticles in saturated porous media: Role of ionic strength and flow rate. Environ. Sci. Tech. 46(7), 4008-4015 (2012)

Tosco, T., Sethi, R.: Transport of non-newtonian suspensions of highly concentrated micro- and nanoscale iron particles in porous media: A modeling approach. Environmental Science and Technology 44(23), 9062-9068 (2010

Vogel, H.J.: A numerical experiment on pore size, pore connectivity, water retention, permeability, and solute transport using network models. Eur. J. Soil Sci. 51(1), 99-105 (2000). doi:10.1046/j.1365-2389.2000.00275.x

Zaretskiy, Y., Geiger, S., Sorbie, K., Förster, M.: Efficient flow and transport simulations in reconstructed 3D pore geometries. Adv. Water Res. 33(12), 1508-1516 (2010)

Zeinijahromi, A., Vaz, A., Bedrikovetsky, P.: Well impairment by fines migration in gas fields. J. Pet. Sci. Eng. (2012)

Zhang, D., Zhang, R., Chen, S., Soll, W.E.: Pore scale study of flow in porous media: Scale dependency, REV, and statistical REV. Geophys. Res. Lett. 27(8), 1195-1198 (2000)

Zhang, Z., Li, J., Zhou, J.: Microscopic Roles of "Viscoelasticity" in HPMA polymer flooding for EOR. Transp. Porous Media 86(1), 199-214 (2011). doi:10.1007/s11242-010-9616-6

Zhong, L., Szecsody, J., Oostrom, M., Truex, M., Shen, X., Li, X.: Enhanced remedial amendment delivery to subsurface using shear thinning fluid and aqueous foam. J. Haz. Mat. 191(1-3), 249-257 (2011)

Figures

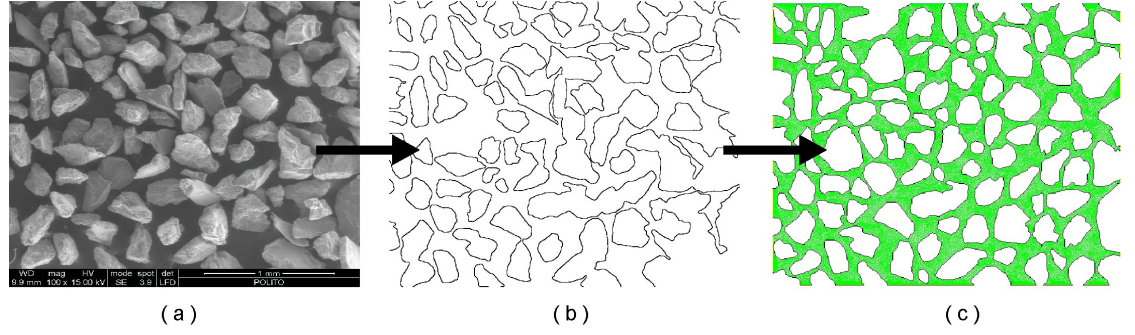(a)   (b)   (c)

Fig. 1 Example of the digitalization process for the construction of the model domains: SEM image of sand grains (a), digitalized contours (b) and computational grid (c).
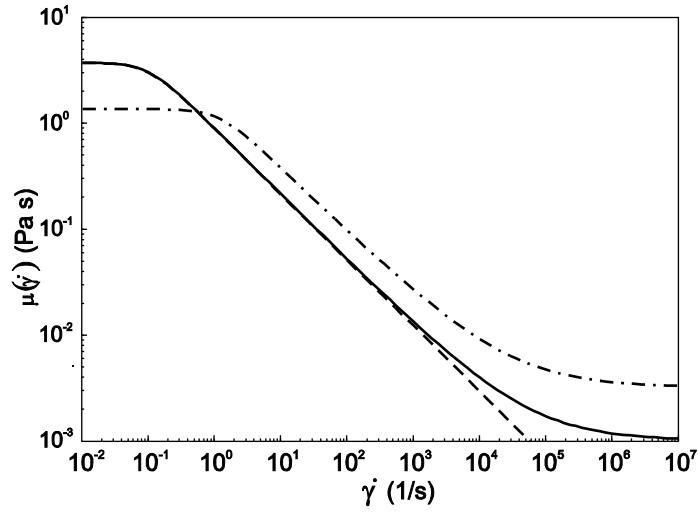

Fig. 2 Model curves for the shear viscosity $\mu\left(\dot{\gamma}\right)$ as a function for shear rate $\dot{\gamma}$ for non-Newtonian shear-thinning fluids used in the micro-scale flow simulations: Cross model (continuous line), Ellis model (dashed line), Carreau model (dash-dotted line). The corresponding equations are reported in Table 2, the coefficients in Table 3.
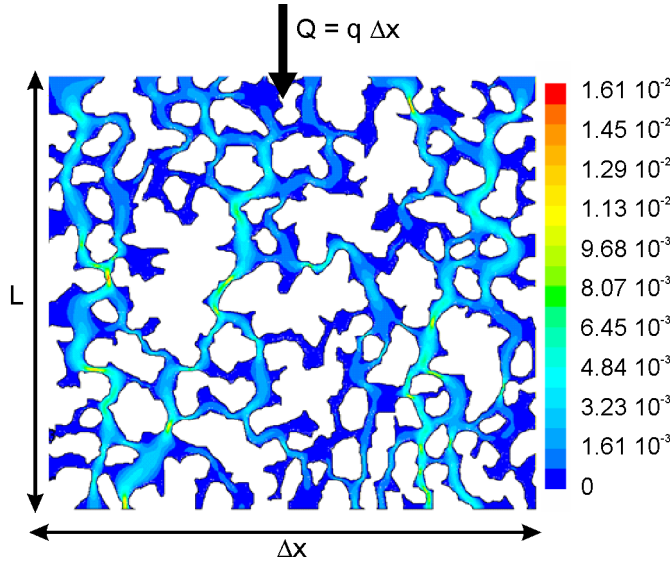
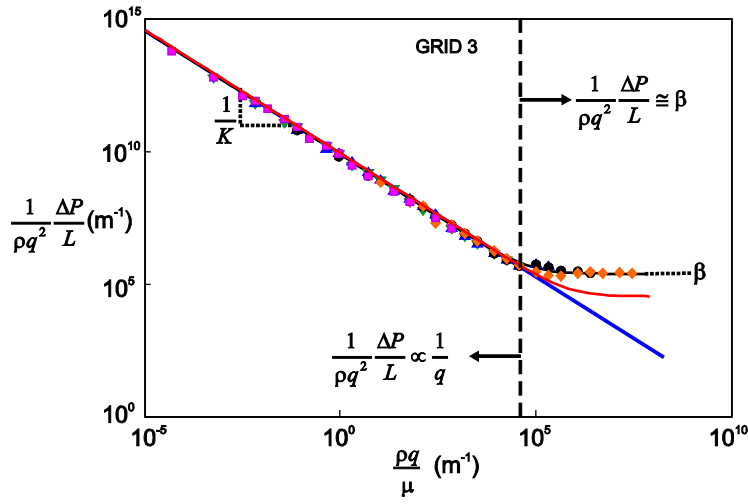**Fig. 3** Velocity magnitude contour plots for a superficial velocity of 10^{-3} m/s for Grid 3.

Fig. 4 Normalized pressure drops versus normalized superficial velocity for Grid 3 for Newtonian viscosity equal to 1×10^{-3} (♦), 1×10^{-2} (●), 1×10^{-1} (▲), 1×10^{0} (■), 1×10^{1} (▼) Pa s. Solid lines represent the Darcy (dotted line) and Darcy-Forchheimer law (solid) calculated via inverse fitting of the simulation results. The generalized Ergun equation (dashed) is also reported.
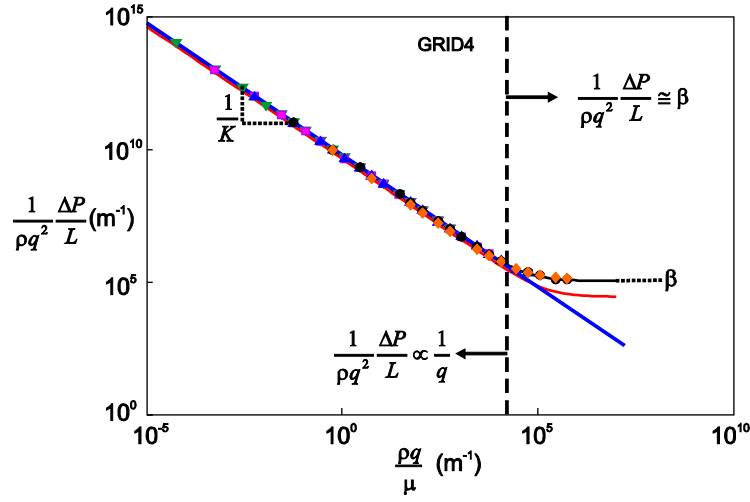
Fig. 5 Normalized pressure drops versus normalized superficial velocity for Grid 4 for Newtonian viscosity equal to 1×10^{-3} (♦), 1×10^{-2} (●), 1×10^{-1} (▲), 1×10^{0} (■), 1×10^{1} (▼) Pa s. Solid lines represent the Darcy (dotted line) and Darcy-Forchheimer law (solid) calculated via inverse fitting of the simulation results. The generalized Ergun equation (dashed) is also reported.
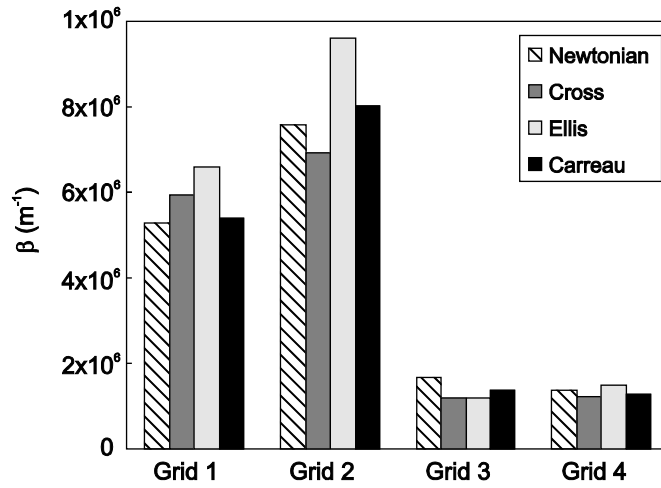

Fig. 6 Comparison of least-square fitted values of the Forchheimer coefficient β reported for each grid and rheological model.
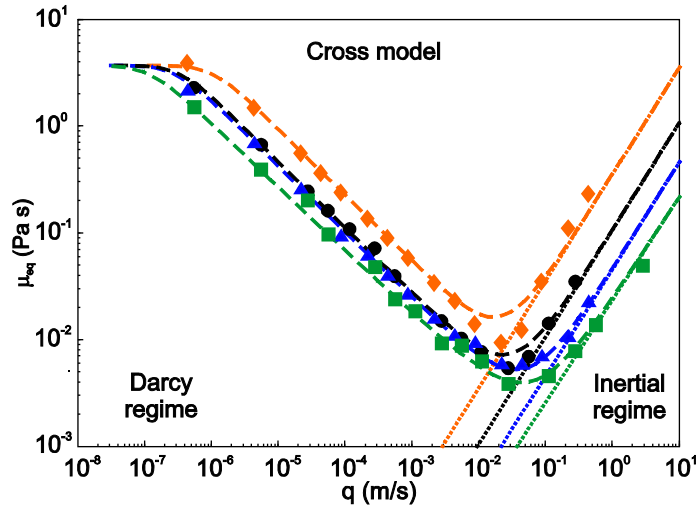
Fig. 7 Data points of equivalent viscosity obtained from micro-scale flow simulations ($\mu_{eq}=K/q\cdot\Delta P/L$) plotted against specific discharge for the Cross rheological model, for Grid 1 (♦), 2 (●), 3 (▲), and 4 (■). The porous medium viscosity $\mu_m(\dot{\gamma}_m)$ (solid line) and inertial term $K\beta\rho q$ (dotted lines) are also reported, calculated using the fitted coefficients
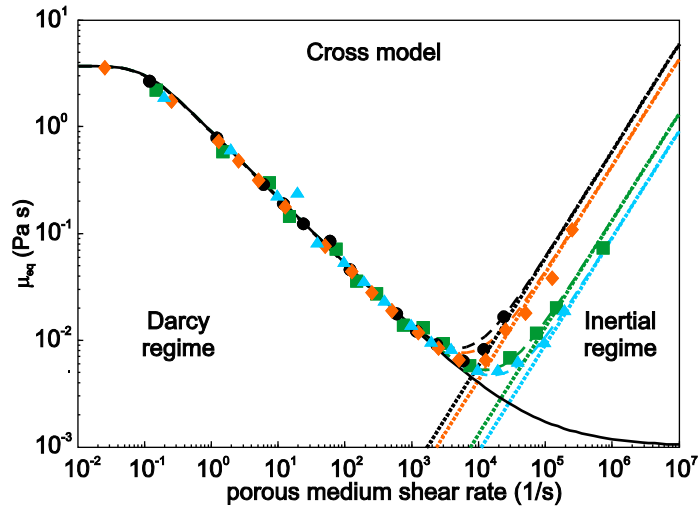

Fig. 8 Data points of equivalent viscosity obtained from micro-scale flow simulations ($\mu_{eq}=K/q\cdot\Delta P/L$) plotted against the porous medium shear rate (eq. 7) for the Cross rheological model, for Grid 1 (♦), 2 (●), 3 (▲), and 4 (■). The equivalent viscosity curve μ_{eq} (dashed lines) obtained via least square fitting of numerical results is also reported, along with its components, namely porous medium viscosity $\mu_m(\dot{\gamma}_m)$ (solid line) and inertial term $K\beta\rho q$ (dotted lines).

Fig. 9 Data points of equivalent viscosity obtained from micro-scale flow simulations ($\mu_{eq}=K/q \cdot \Delta P/L$) plotted against the porous medium shear rate (eq. 7) for the Ellis rheological model, for Grid 1 (♦), 2 (●), 3 (▲), and 4 (■). The equivalent viscosity curve μ_{eq} (dashed lines) obtained via least square fitting of numerical results is also reported, along with its components, namely porous medium viscosity $\mu_m(\dot{\gamma}_m)$ (solid line) and inertial term $K\beta\rho q$ (dotted lines).

Fig. 10 Data points of equivalent viscosity obtained from micro-scale flow simulations ($\mu_{eq}=K/q \cdot \Delta P/L$) plotted against the porous medium shear rate (eq. 7) for the Carreau rheological model, for Grid 1 (♦), 2 (●), 3 (▲), and 4 (■).The equivalent viscosity curve μ_{eq} (dashed lines) obtained via least square fitting of numerical results is also reported, along with its components, namely porous medium viscosity $\mu_m(\dot{\gamma}_m)$ (solid line) and inertial term $K\beta\rho q$ (dotted lines).
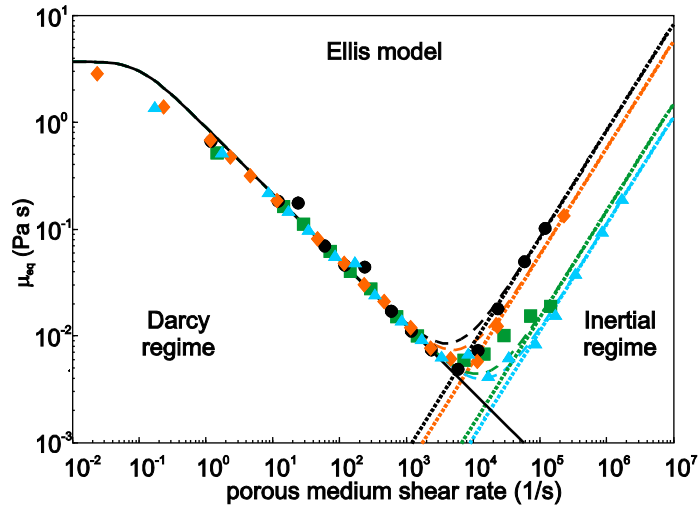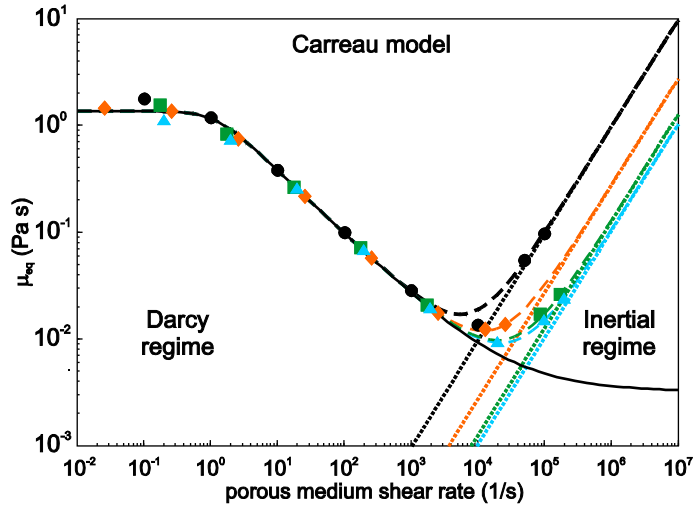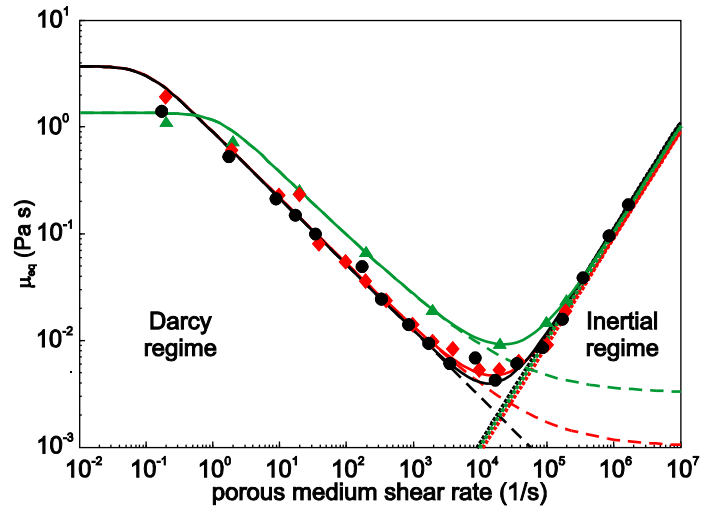
Fig 11 Data points of equivalent viscosity and least-squares fitted viscosity curves (solid lines) for Cross (♦), Ellis (●) and Carreau (▲) models on Grid 3. The two components of the equivalent viscosity are also reported, namely porous medium viscosity $\mu_m(\dot{\gamma}_m)$ (dashed lines) and inertial term $K\beta\rho q$ (dotted lines).

Tables

Table 1: Rheological models used for numerical flow simulations of non-Newtonian fluids.

Rheological model	Bulk viscosity	Equivalent viscosity
Power law	$\mu\left(\dot{\gamma}\right) = C\dot{\gamma}^{\,n-1}$	$\mu_{eq} = C\dot{\gamma}^{\,n-1} + \beta\rho K|q|$
Cross	$\mu\left(\dot{\gamma}\right) = \mu_\infty + \dfrac{\mu_0 - \mu_\infty}{1+\left(\lambda\dot{\gamma}\right)^\chi}$	$\mu_{eq} = \mu_\infty + \dfrac{\mu_0 - \mu_\infty}{\left[1+\left(\dfrac{\lambda\alpha}{\sqrt{K\varepsilon}}\right)^\chi|q|^\chi\right]} + \beta\rho K|q|$
Ellis	$\mu\left(\dot{\gamma}\right) = \dfrac{\mu_0}{1+\left(\lambda\dot{\gamma}\right)^\chi}$	$\mu_{eq} = \dfrac{\mu_0}{1+\left(\lambda\dot{\gamma}\right)^\chi} + \beta\rho K|q|$
Carreau	$\mu\left(\dot{\gamma}\right) = \mu_\infty + \dfrac{\mu_0 - \mu_\infty}{\left[1+\left(\lambda\dot{\gamma}\right)^2\right]^{\chi/2}}$	$\mu_{eq} = \mu_\infty + \dfrac{\mu_0 - \mu_\infty}{\left[1+\left(\lambda\dot{\gamma}\right)^2\right]^{\chi/2}} + \beta\rho K|q|$

Table 2: Porosity ε, specific surface area a and grid size for all geometries investigated. Porosity is calculated as the ratio of the void to the total volume of the grid domain. Specific surface area is calculated as the ratio of the solid-liquid interface area to the volume of the solid.

Grid label	Grid parameters		Grid size		
	ε (-)	a (m^{-1})	x (m)	y (m)	number of cells in pore space
Grid 1	0.51	5.47×10^3	0.010	0.008	1.79×10^5
Grid 2	0.49	1.05×10^4	0.003	0.003	8.78×10^4
Grid 3	0.41	7.78×10^3	0.007	0.006	1.75×10^5
Grid 4	0.49	1.09×10^4	0.010	0.008	2.21×10^5

Table 3: Values of the curve parameters for Cross, Ellis and Carreau rheological models used in micro-scale flow simulations.

Rheological model	Parameters			
	μ_∞ (Pa s^{-1})	μ_0 (Pa s^{-1})	λ (-)	χ (-)
Cross	1.0×10^{-3}	3.52	10.1	0.62
Ellis	-	3.52	10.1	0.62
Carreau	3.2×10^{-3}	1.35	0.85	0.60

Table 4: Parameters K, β, α calculated for the four grids from Ergun equation (Eq. 4) and obtained from inverse modeling of flow simulation results with the Darcy-Forchheimer's law (Eq. 2) for Newtonian and non-Newtonian fluids (Cross, Ellis and Carreau rheological models).

Grid	Parameter	Ergun (Newtonian fluids)	Darcy-Forchheimer			
			Newtonian fluids	Cross fluid	Ellis fluid	Carreau fluid
1	K (m^2)	1.23×10^{-9}	5.98×10^{-10}	5.98×10^{-10} *(not fitted)*		
	β (m^{-1})	1.12×10^4	5.28×10^5	5.94×10^5	6.59×10^5	5.40×10^5
	α (-)	-	-	1.60	1.70	1.75
2	K (m^2)	2.55×10^{-10}	1.54×10^{-10}	1.54×10^{-10} *(not fitted)*		
	β (m^{-1})	2.61×10^4	7.59×10^5	6.92×10^5	9.61×10^5	8.04×10^5
	α (-)	-	-	2.48	2.56	2.55
3	K (m^2)	2.63×10^{-10}	3.91×10^{-10}	3.91×10^{-10} *(not fitted)*		
	β (m^{-1})	3.42×10^4	1.67×10^5	1.18×10^5	1.20×10^5	1.37×10^5
	α (-)	-	-	4.17	4.18	4.09
4	K (m^2)	2.35×10^{-10}	1.82×10^{-10}	1.82×10^{-10} *(not fitted)*		
	β (m^{-1})	2.74×10^4	1.37×10^5	1.29×10^5	1.32×10^5	1.37×10^5
	α (-)	-	-	5.26	4.70	4.67